SPECIAL
Connecting the Tropics to the Polar Regions
COLLECTION

Accumulation Variability in the Antarctic Peninsula: The Role of Large-Scale Atmospheric Oscillations and Their Interactions*

BRADLEY P. GOODWIN+ AND ELLEN MOSLEY-THOMPSON

Byrd Polar and Climate Research Center, and Department of Geography (Atmospheric Sciences Program), The Ohio State University, Columbus, Ohio

AARON B. WILSON, STACY E. PORTER, AND M. ROXANA SIERRA-HERNANDEZ

Byrd Polar and Climate Research Center, The Ohio State University, Columbus, Ohio

(Manuscript received 15 May 2015, in final form 28 November 2015)

ABSTRACT

A new ice core drilled in 2010 to bedrock from the Bruce Plateau (BP) on the Antarctic Peninsula (AP) provides a high temporal resolution record of environmental conditions in this region. The extremely high annual accumulation rate at this site facilitates analysis of the relationships between annual net accumulation A_n on the BP and large-scale atmospheric oscillations. Over the last ~45 years, A_n on the BP has been positively correlated with both the southern annular mode (SAM) and Southern Oscillation index (SOI). Extending this analysis back to 1900 reveals that these relationships are not temporally stable, and they exhibit major shifts in the late-1940s and the mid-1970s that are contemporaneous with phase changes in the Pacific decadal oscillation (PDO). These varying multidecadal characteristics of the A_n–oscillation relationships are not apparent when only data from the post-1970s era are employed. Analysis of the longer ice core record reveals that the influence of the SAM on A_n depends not only on the phase of the SAM and SOI but also on the phase of the PDO. When the SAM's influence on BP A_n is reduced, such as under negative PDO conditions, BP A_n is modulated by variability in the tropical and subtropical atmosphere through its impacts on the strength and position of the circumpolar westerlies in the AP region. These results demonstrate the importance of using longer-term ice core–derived proxy records to test conventional views of atmospheric circulation variability in the AP region.

1. Introduction

The Antarctic Peninsula (AP) is a climatologically complex region that includes ice-free ocean, sea ice, land ice, and significant topographic relief within a relatively small area (Fig. 1). Air temperatures have increased, particularly along the west coast since the 1950s (e.g., ~2.5°C; King 1994), reflecting one of the strongest positive regional trends recorded globally (Marshall et al. 2002; Turner et al. 2005). Rapid warming observed over the AP has been associated with the strengthening of the circumpolar westerly winds primarily driven by anthropogenic forcing (Marshall et al. 2006). Enhanced advection of warmer maritime air masses over the orographic barrier of the AP and the resulting foehn winds warm the cooler continental climate on the east side (Orr et al. 2004; Marshall et al. 2006). Disintegration of ice shelves has progressed southward (Scambos et al. 2004) from the northern tip as predicted by Mercer (1978) to occur in response to the anticipated warming of the planet due to increasing greenhouse gas emissions.

However, many factors have been identified as drivers of recent AP/West Antarctic climate change including tropical variability (Ding et al. 2011; Schneider et al. 2012; Ding and Steig 2013; Clem and Fogt 2015), anomalous sea ice concentrations (Ding and Steig 2013), and Amundsen Sea low (ASL) variability (Fogt et al. 2012; Turner et al. 2013; Hosking et al. 2013; Clem and Fogt 2013). All of these factors have demonstrated highly regional and seasonal impacts on the climate of the AP and West

* Byrd Polar and Climate Research Center Contribution Number 1443.

+ Current affiliation: Senior Service Fellow at the Agency for Toxic Substances and Disease Registry.

Corresponding author address: Ellen Mosley-Thompson, Byrd Polar and Climate Research Center, The Ohio State University, 108 Scott Hall, 1090 Carmack Rd., Columbus, OH 43210.
E-mail: thompson.4@osu.edu

DOI: 10.1175/JCLI-D-15-0354.1

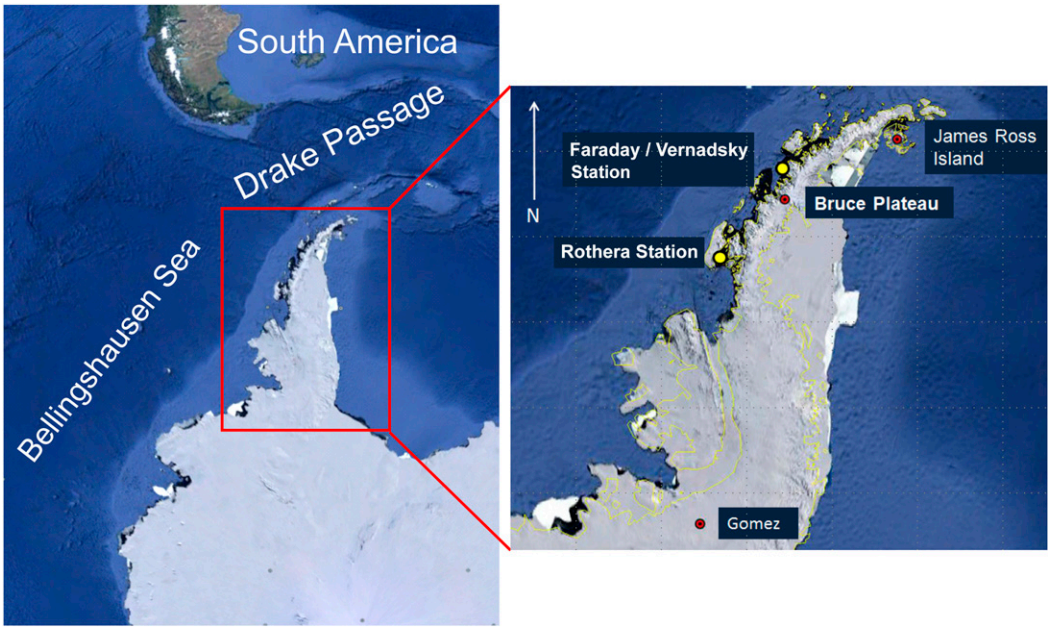

FIG. 1. Location of the sites in the AP discussed in the paper.

Antarctica. These processes are linked to large-scale atmospheric oscillations, which are important determinants of both weather and climate in this region.

One of the primary controls on southern high-latitude climate is the southern annular mode (SAM) (e.g., Thompson and Wallace 2000), defined by Gong and Wang (1999) as the difference in zonal mean sea level pressure (MSLP) between 40° and 65°S. The positive (negative) phase of the SAM is marked by high (low) pressure anomalies in the midlatitudes and low (high) pressure anomalies across the high latitudes and Antarctica, which result in a stronger (weaker) than normal and contracted (relaxed) circumpolar westerly wind belt. Both the sign and magnitude of the SAM exert control on Southern Hemisphere (SH) climate variations including sea ice extent and precipitation (Kang et al. 2011; Simpkins et al. 2012). Since the 1970s, the SAM has been steadily trending toward positive values, and over the last decade it has been more consistently positive (Thompson and Solomon 2002; Marshall 2003a; Thompson et al. 2011). Positive SAM values are correlated with colder temperatures over most of Antarctica, with the exception of the AP, where warmer temperatures prevail (Marshall 2002; Schneider et al. 2004).

El Niño–Southern Oscillation (ENSO) (Trenberth 1997), a global ocean–atmosphere phenomenon originating in the tropical Pacific basin, is associated with teleconnections (linkages) to many parts of the globe including Antarctica (Turner 2004; Fogt and Bromwich 2006; Gregory and Noone 2008; Stammerjohn et al. 2008; Fogt et al. 2011). Physically, ENSO imparts a strong influence on the climate of the AP through the South Pacific convergence zone (SPCZ), an area of low-level convergence, clouds, and precipitation that extends from New Guinea southeast toward French Polynesia (30°S, 120°W) (Vincent 1994). Recent austral spring [September–November (SON)] trends in MSLP in the southwest Atlantic Ocean associated with ENSO variability (La Niña) have been linked to warming temperatures across the northwest AP (Clem and Fogt 2015).

The strength of the ENSO teleconnection to the high-latitude South Pacific and resultant SAM–tropical sea surface temperature (SST) relationship is modulated by the sign and strength of individual SAM events (Fogt and Bromwich 2006; L'Heureux and Thompson 2006; Fogt et al. 2011; Clem and Fogt 2013) with preferences for in-phase coupling between the phenomena (positive SAM/La Niña and negative SAM/El Niño) (Gong et al. 2010, 2013; Fogt et al. 2011; Ding et al. 2012). The climate of the AP is therefore influenced by this coupling between the SAM and ENSO. While a positive SAM exhibits lower pressure near the Antarctic continent and stronger high-latitude circumpolar westerlies, the SPCZ is oriented southwest of climatology during cool ENSO (La Niña) events (Vincent 1994). This generates a positive feedback with poleward transient eddy momentum flux that interacts with the polar front to increase cyclonic activity in the South Pacific sector of the Antarctic coast (Chen et al. 1996). Conversely, during negative SAM the circumpolar trough is weakened as the high-latitude storm track relaxes to the north while warm ENSO (El Niño) events shift the SPCZ equatorward as well, directing

cyclones away from the AP and toward South America (Fogt 2007; Eichler and Gottschalck 2013). Thus, the combination of the SAM and ENSO and their associated modulation of SH storm tracks (Fogt et al. 2011; Schneider et al. 2012) influence accumulation on the AP.

In addition to the SAM and ENSO, the Pacific decadal oscillation (PDO) also influences the climate of the AP. Often described as ''ENSO like'' decadal-scale variability in the North Pacific (Zhang et al. 1997), Mantua et al. (1997) coined the term ''PDO'' to describe an interdecadal ocean–atmosphere pattern of anomalous SSTs and MSLP observed in the North Pacific that strongly impacts salmon populations. Unlike ENSO, the most distinctive oceanic–atmospheric footprint of the PDO is located in the North Pacific Ocean, where the positive phase denotes warm (cool) SST anomalies in the eastern (western) Pacific (with opposite SST anomalies during negative PDO conditions). In fact, the PDO has been shown to respond to many factors including stochastic atmospheric processes, SST anomaly reemergence in subsequent winters, and ENSO through both the atmospheric bridge (Rossby waves) and oceanic wave processes (e.g., Alexander et al. 1999; Newman et al. 2003; Schneider and Cornuelle 2005). The PDO has changed polarity in 1925, 1947, and 1977 CE (Common Era; henceforth all dates are in CE although not designated as such) with the period prior to 1925 characterized as a ''warm'' PDO phase. The ''cool'' phase observed between 1947 and 1977 resulted in more prevalent La Niña–like teleconnection patterns while the warm post-1977 phase enhanced the frequency of El Niño–like patterns. In the late 1990s, the PDO began trending negative specifically during SON, which has been independently linked to a deepening of the ASL, hence impacting temperatures in West Antarctica, and to a lesser degree in the AP (Clem and Fogt 2015).

The PDO shares a common North Pacific signature with the interdecadal Pacific oscillation (IPO) (e.g., Folland et al. 1999; Power et al. 1999), a phenomenon of SST and atmospheric circulation variability shown to quasi-independently impact the SPCZ (Folland et al. 2002) and thus, SH climate. Many authors suggest that the PDO and the IPO are relatively equivalent in describing Pacific-wide ocean–atmosphere climate variability (Folland et al. 2002; Deser et al. 2004; Dong and Dai 2015), but this remains an active area of research inquiry. However, similar tropically driven variability associated with the PDO and IPO has been demonstrated to drive both NH and SH climate variability on interdecadal time scales. Evidence strongly supports a northward displacement of the SPCZ from the long-term mean during both the warm phase of ENSO (Vincent 1994) and ENSO-like (PDO/IPO) variability (Garreaud and Battisti 1999; Folland et al. 2002). This coincides with the eastward shift of warmer SSTs and deep convection in the central and eastern tropical Pacific. This alters the atmospheric heating anomalies that are dynamically tied to the generation of Rossby waves and teleconnections throughout both the NH and SH (Sardeshmukh and Hoskins 1988; Lee et al. 2009).

Therefore, the change in the location of the SPCZ is a primary mechanism through which tropical climate variability is transmitted to higher latitudes in the SH. The direct impacts of shifting the SPCZ on SSTs, SLP, temperature, and precipitation across the midlatitudes and tropical land areas of the SH have been documented (e.g., Andreoli and Kayano 2005; Dong and Dai 2015). The impacts extend to higher latitudes; for example, Garreaud and Battisti (1999) address directly the impacts of ENSO-like variability on the Bellingshausen Sea region. Clem and Renwick (2015) demonstrate that spring temperature trends over West Antarctica and the AP for the period 1979–2014 are also related to an increase in deep tropical convection along the poleward side of the SPCZ, resulting from low-level wind convergence and increases in SLP in the eastern Pacific.

Thus, the climate of this region reflects complex interactions among natural and anthropogenic forcing including those associated with stratospheric ozone depletion/recovery and increasing greenhouse gas concentrations (Thompson and Solomon 2002). There is also strong evidence for both regional (Silvestri and Vera 2009) and continent-wide (Marshall et al. 2013) reversals in the relationship between the SAM and Antarctic temperatures that indicates that the SAM's influence on the climate of Antarctica is nonstationary in time. Their results suggest a limitation on the ability to derive a proxy for the SAM directly from a single Antarctic ice core. The results reported here demonstrate that the Antarctic climate and its relationship to the SAM and ENSO appear to be interdependent on the PDO, which provides additional links between the northern/tropical Pacific Ocean and the Southern Ocean and hence the AP. Changes to the atmospheric and oceanic teleconnections during different phases of these indices impact the climate of the AP, which provides an opportunity to further examine these interactions. Fortunately, from a continental perspective, the AP contains the greatest abundance of climate records based on direct meteorological observations with some extending well into the 1940s and one (i.e., Orcadas) extending to the beginning of the twentieth century (Turner et al. 2004). Two major climatic variables, air temperature and precipitation, can be reconstructed over long time periods from ice core–derived proxies as well.

There is abundant evidence from ice cores (Thompson et al. 1994; Thomas et al. 2008, 2009; Abram et al. 2010, 2011; Mulvaney et al. 2012), model simulations (Hansen et al. 1999; Dethloff et al. 2010), and reanalysis data (Sime et al. 2009) of rapid climate changes in the AP. Here we exploit a new annually resolved ice core record of accumulation from the Bruce Plateau (BP) in the AP. Accumulation represents an integrated climate signal of the thermodynamic properties of temperature and moisture and influences the chemical composition of snowfall that is preserved as ice and used for paleoclimate reconstruction. This longer-term record extends observational records and provides an opportunity to better understand climate variability in the AP over the last century. However, the forces driving it vary spatially and temporally and lead to complex interactions. Furthermore, while reanalysis and model data have been used to draw seasonal links between tropical variability and the AP in the post-1979 period, the focus of this study is on the annual relationships discernible from the BP core over the last century. Section 2 presents the data and methods used in this paper while section 3 discusses the role of various atmospheric oscillators in modulating the variability of accumulation (precipitation) over the BP. Section 4 provides a discussion of these linkages and highlights the importance of understanding them and their interactions, while section 5 presents the conclusions of this research.

2. Data and methods

a. *Annually resolved ice core proxy data from the Bruce Plateau*

A new ice core from the AP, the first from the BP, provides an excellent opportunity to deepen our understanding of climate variability in the region, especially along the northwestern coast (Fig. 1). This core, henceforth the BP core, is 448.12 m long and was drilled in 2010 through the BP ice field [66.03°S, 64.07°W; 1975.5 m above mean sea level (MSL)] to bedrock. The west coast of the AP is dominated by westerly maritime flow from the Southern Ocean and/or South Pacific while the east coast is dominated by continental flow from the Antarctic interior (Turner et al. 2002). The result is much warmer temperatures and more precipitation along the west coast and colder, drier conditions along the east coast. The crest of the AP acts as a topographic divide separating the two regions. The BP ice field feeds glaciers flowing into the Larsen Ice Shelf to the east and into numerous bays, including Barilari Bay on the west. Very high accumulation along the west coast of the AP results in a strong westward displacement of the BP ice divide so that it is in close proximity to Barilari Bay. The BP ice core was drilled slightly east (~2 km) of this topographic divide where the basal topography is smoother. The extremely high accumulation rate observed during the drilling campaign and later determined from the analysis of the BP core indicates that the site experiences predominantly westerly maritime flow and thus is ideally situated to capture the precipitation (and its constituents) reflecting climate variability over the Bellingshausen Sea (Fig. 1). This annual net accumulation [1.84 m of water equivalent (w.e.) per year from 1900 to 2009] ensures a high-resolution proxy climate history. It is essential that the BP ice core time scale be precise for the period encompassed by this study (1900–2009) because the annually resolved ice core–derived proxy climate variables are compared with atmospheric and/or oceanic observations that are aggregated into annual averages.

The concentration of methanesulfonic acid (MSA) measured by ion chromatography (Dionex ICS-3000) has been shown at other Antarctic coastal ice core sites to vary seasonally, with a summer maximum and winter minimum (Curran and Jones 2000; Curran et al. 2003; Preunkert et al. 2007; Abram et al. 2013). The seasonality reflects changes in biological productivity over the course of the year, which makes it an excellent chemical species for the construction of an extremely robust time scale for the BP core (Fig. 2). In addition, the elevated concentrations of gross beta radioactivity (Fig. 2b) from thermonuclear testing arrived in Antarctica in 1964/65 (Crozaz 1969; Pourchet et al. 1983) and provide additional confidence in the time scale. Annually averaged ice core data are assumed to correspond approximately to calendar years, but uncertainty in the timing of the austral summer maxima, identified by the seasonal peak concentration of MSA, results in an uncertainty of approximately two months in the break between years.

The reconstructed annual net accumulation A_n and oxygen isotopic ratio ($\delta^{18}O$) provide proxy-based histories of precipitation and temperature, respectively. The Dansgaard and Johnsen (1969) model was used to reconstruct the original thicknesses of the annual layers (i.e., A_n) at depth in the BP core. Analysis of $\delta^{18}O$ was performed with a Picarro Cavity Ring-Down Spectrometer, Model L2120-i ($\delta^{18}O$ precision: 0.05‰). The BP A_n and $\delta^{18}O$ records from 1900 to 2009 have a time scale uncertainty of less than one year and are contained in the upper 194.23 m of the core, or roughly the upper half of the BP ice sheet. The precise time scale for A_n coupled with its high interannual variability ($\sigma = \pm 0.56$ m w.e.) makes this an ideal site for exploring how large-scale circulation patterns affect accumulation in this region.

b. *Southern annular mode*

Several authors have created SAM indices of various lengths back in time, although results in this

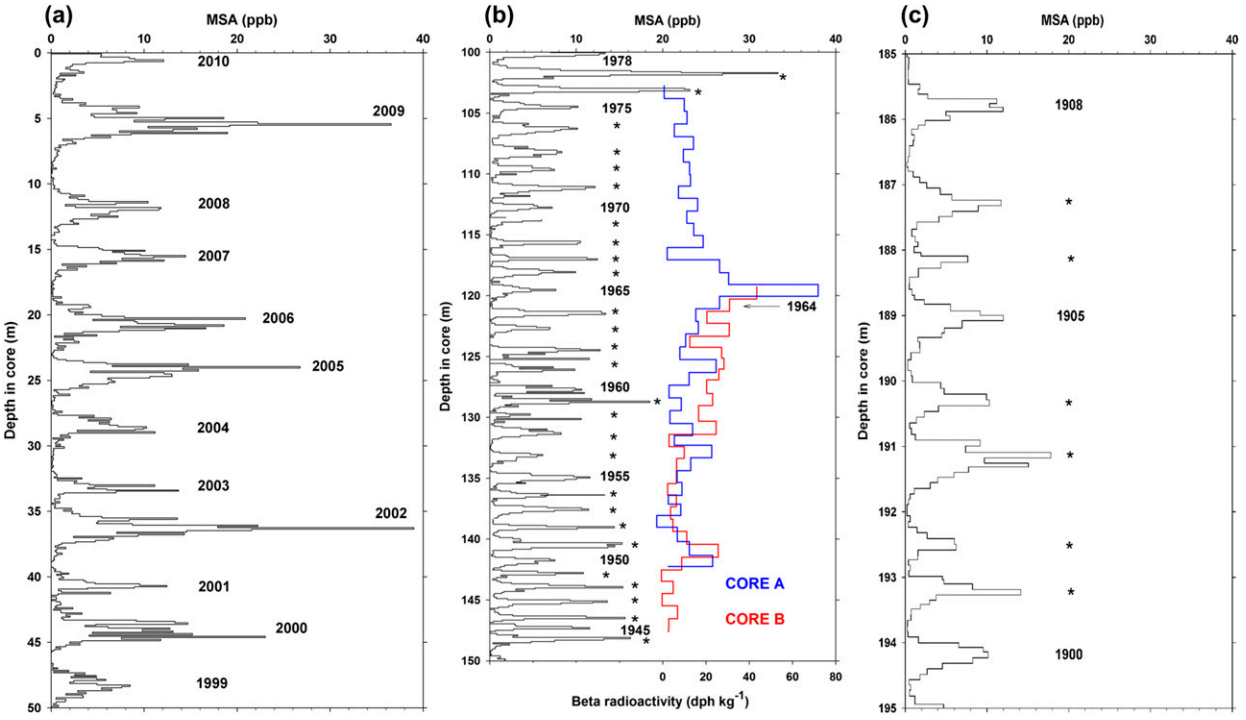

FIG. 2. Seasonal variations in the concentration of MSA used to date the BP ice core: (a) the initial 11 years contained in the upper 50 m of the core, (b) the section of the core containing the 1964 beta radioactivity horizon, and (c) the first 8 years of the twentieth century contained in ~10 m of core. Comparison of (a) and (c) illustrates the thinning of the annual layers with depth.

investigation will focus mainly on two: the Marshall SAM index (Marshall 2003a,b) and the Fogt reconstructed SAM index (Fogt 2009; Fogt et al. 2009; Jones et al. 2009). The annual (January–December) Marshall index (1957–2009) is calculated using the monthly values provided by Marshall (2003b). The Fogt index (Fogt 2009) extends from 1905 to 2005 with annual (December–November) values constructed from the seasonal resolution. The Jones reconstruction (Jones et al. 2009; provided by Julie Jones to Aaron Wilson on 18 April 2014) uses the first principal component of extratropical sea level pressure (SLP) as the predictand, while the Fogt reconstruction uses the Marshall index, which is based on station SLP. Visbeck (2007, 2009) reconstructed Antarctic SLP variability by assuming atmospheric mass conservation between Antarctica (data very scarce) and the subtropical latitudes (more data available) and has been shown to be less reliable than other reconstructions in all seasons except austral summer (Jones et al. 2009). A recently reconstructed SAM index (Abram et al. 2014a,b) uses a suite of proxy records from South America and Antarctica plus a new ice core–derived temperature record [inferred from deuterium (δD)] recovered in 2008 from James Ross Island (Fig. 1) on the eastern side of the northern tip of the AP. Finally, the much shorter SAM record from the National Oceanic and Atmospheric Administration (NOAA) (Mo 2000; NOAA 2000) is included for comparison over the very recent period.

c. *Southern Oscillation index*

The Southern Oscillation index (SOI), the atmospheric component of ENSO, is measured as the difference in SLP between Tahiti and Darwin (Ropelewski and Jones 1987; Allan et al. 1991; Können et al. 1998). SOI data, available at monthly resolution (Climatic Research Unit 1987) from 1866 to the present, were annually averaged on a calendar year basis for this comparison.

d. *Pacific decadal oscillation*

The PDO describes SSTs in the North Pacific Ocean and shows significant decadal variability (Mantua et al. 1997). The PDO index is determined by the first principal component of SST anomalies in the Pacific Ocean north of 20°N. Data for the PDO were obtained from Mantua (1997) for the period between 1900 and 2009 at monthly resolution and averaged to annual resolution on a calendar year basis.

e. *TransPolar Index*

The TransPolar Index (TPI) (Pittock 1980, 1984; Jones et al. 1999) is a low-frequency movement in the phase of

wavenumber 1 around the SH, which is expressed as an oscillation in troughing/ridging between New Zealand and South America. Monthly data, calculated as the normalized pressure difference between Hobart, Australia (43°S, 147°E) and Stanley, Falkland Islands (52°S, 58°W), were obtained from the Climatic Research Unit (1980) and averaged over the calendar years for 1905–2004.

f. *Gridded meteorological data*

Global SSTs are available from NOAA's Extended Reconstructed SST, version 3b (ERSST.v3b; Smith and Reynolds 2002). The SSTs are based on in situ data and are aggregated monthly from January 1854 to the present on a 2° × 2° grid (Xue et al. 2003; Smith et al. 2008). The monthly data were averaged over calendar years for 1900–2009 for comparison with the BP ice core accumulation. Interpolated outgoing longwave radiation (OLR) data are from NOAA's Climate Data Record Program on a 1° × 1° grid from satellite observations from 1979 to 2012 (Lee 2014). Monthly SLP data were acquired from the National Centers for Environmental Prediction (NCEP)–National Center for Atmospheric Research (NCAR) reanalyses for 1979–2012 (Kalnay et al. 1996).

g. *Station temperature data*

Annual temperature data are provided by the Scientific Committee on Antarctic Research (SCAR) Reference Antarctic Data for Environmental Research (READER) project for two stations, Faraday/Vernadsky and Rothera (SCAR 2004; Turner et al. 2004). Temperature records from Faraday/Vernadsky (65.4°S, 64.4°W; 11 m MSL) begin in 1947 and from Rothera (67.5°S, 68.1°W; 32 m MSL) begin in 1976.

h. *Changepoint analysis*

A key challenge in changepoint analysis is the ability to detect multiple changes within a given time series or sequence. The changepoints in the time series of the 11-yr running correlations between A_n and the Fogt SAM index were calculated using the R changepoint package presented by Killick and Eckley (2014). The pruned exact linear time algorithm was used to identify times when a change occurred in the mean of the 11-yr running correlation between accumulation and the SAM index. The number of changepoints identified is determined using the Bayesian information criterion to prevent overfitting of the model.

3. Accumulation variability on the AP and the role of large-scale atmospheric oscillators

Temperature and precipitation are typically used to characterize regional climate variability and where these records are short, as in the AP, longer proxy records of temperature and precipitation are inferred from oxygen and hydrogen isotopic ratios (δ^{18}O and δD) and A_n, respectively. The annual net accumulation reflects the integrated contributions of precipitation, sublimation, wind scouring, and redeposition. Accumulation rates measured in AP ice cores have increased over the last century and most dramatically since about 1950 (Thomas et al. 2008) in concert with a contemporaneous increase in temperature. Figures 3a and 3b confirm that the BP has experienced an increase in annual net accumulation over the twentieth century (0.102 m w.e. decade^{-1}) with enhanced accumulation (0.193 m w.e. decade^{-1}) since 1950 that is concomitant with warming temperatures at the two nearest meteorological stations (Faraday/Vernadsky and Rothera). Interestingly, the δ^{18}O record reflects only a modest ^{18}O enrichment (0.065‰ decade^{-1}) over the twentieth century with a larger warming trend (0.157‰ decade^{-1}) since 1975 (Fig. 3c). This suggests that in addition to local near-surface temperatures other processes, for example those influenced by tropical climate variability, may also exert control on the isotopic signature of the water vapor.

The recent increase in precipitation on the AP has been linked to the increasing positive trend in the SAM index, which enhances westerly winds and cyclonic activity in this region. Fogt (2007) used outgoing longwave radiation and atmospheric moisture measurements between 1971 and 2000 to identify the location of the predominant SH storm tracks under different SAM and ENSO conditions. His analysis showed that under positive (negative) SAM conditions, enhanced (reduced) cyclonic activity in the southern high latitudes leads to an increase (decrease) in atmospheric moisture, and hence precipitation, in regions close to the Antarctic coast. No analysis of the effects of the PDO on SH storm tracks was included by Fogt (2007), likely because the PDO was in a persistent positive phase for nearly the entire analysis window (1971–2000).

The Marshall SAM index extends back to 1957 and is considered the most robust of the available indices (section 2b). Proxy records are generally calibrated to this index, but this implies that their relationship is stationary over the entire reconstructed record. Examination of the available ice core proxy data and their relationship to the Marshall SAM index reveals that the strength of the relationship varies with the specific proxy and the location of the ice core. For example, Abram et al. (2014a) found a strong relationship between the Marshall SAM index and δD from the James Ross Island ice core (Fig. 1). Thomas et al. (2008) report a dramatic increase in accumulation recorded in the Gomez ice core (Fig. 1) from the 1960s onward that is correlated with the SAM. On the BP, A_n, rather than δ^{18}O, is more strongly correlated with the SAM. This

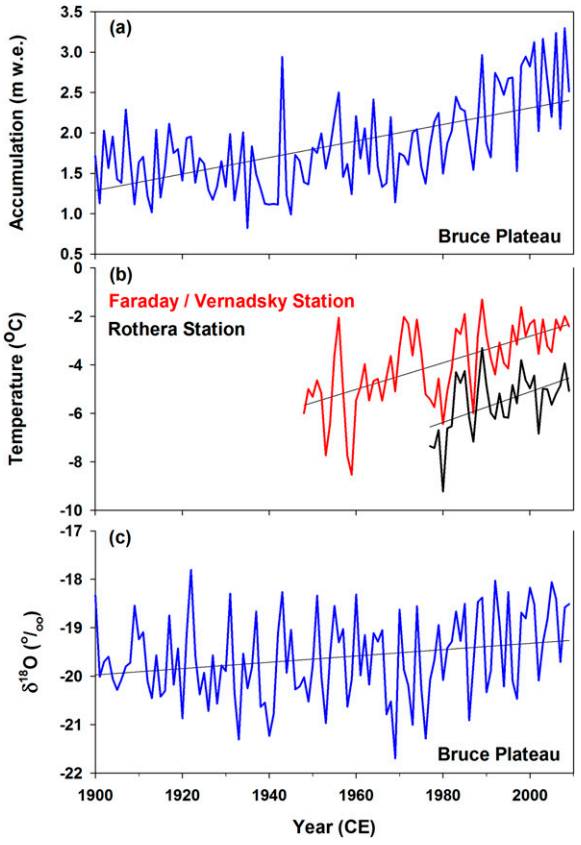

FIG. 3. (a) Annual net accumulation (m w.e.) from 1900 to 2009 reconstructed from the BP ice core. (b) Annual temperatures (and trend) for the full records available from Faraday/Vernadsky Station (red) and Rothera Station (black) along the northwestern coast of the AP (Fig. 1). (c) Annual average $\delta^{18}O$ from 1900 to 2009 reconstructed from the BP ice core.

is demonstrated by comparing the annual values of A_n and $\delta^{18}O$ from the BP ice core with the Marshall SAM and Fogt SAM indices (Fig. 4) for the post-1970 period. This period is identified by the year (1971) in which the maximum running correlation is attained and after which the correlation steadily declines. Figures 4a and 4b reveal a strong positive and statistically significant relationship between A_n on the BP and both the Marshall and Fogt SAM indices from 1971 to 2009 (Marshall: correlation coefficient $r = 0.506, p < 0.001$; Fogt: $r = 0.511$, $p = 0.002$). Figures 4c and 4d reveal a positive but weaker relationship between $\delta^{18}O$ on the BP and both the Marshall and Fogt SAM indices (Table 1). All correlations are based on detrended data, and significance is determined using a two-tailed Student's t test. These results suggest that the ice core–derived A_n record from the BP might provide a proxy for the sign and strength of the SAM, particularly over longer (pre 1900) time scales. However, extending the analysis to 1957 reveals a weakening of the relationship between A_n and $\delta^{18}O$ to both SAM indices (Figs. 4a,b and 4c,d, respectively). This suggests that, prior to 1971, processes in addition to the SAM were influencing both A_n and $\delta^{18}O$. Investigating this further reveals that the A_n–SAM relationship changes sign between 1957 and 1970 (Marshall: $r = -0.13$, $p = 0.656$; Fogt: $r = -0.20$, $p = 0.489$), which accounts for the weaker r values for the post-1957 period. These r values are not statistically significant and thus the sign change could result by chance. However, we argue that the marked change in the sign of the correlation between A_n and the SAM for the pre-1971 period warrants further examination for two important reasons.

The first reason is related to the well-known transition or shift in the mid-1970s of the PDO from a cool phase to a warm phase. The cool phase (1947–77) exhibits a La Niña–like teleconnection pattern with cooler SSTs in the tropical eastern Pacific (Zhang et al. 1997). During La Niña conditions the SPCZ shifts farther southwest directing storms into the South Pacific, where poleward eddy flux momentum may interact with the polar front and intensify cyclonic activity along the South Pacific sector of the Antarctic coast (Chen et al. 1996). The second reason stems from the reliance on the full (1957 onward) Marshall SAM record by studies investigating relationships between the SAM and other proxy climate variables (Thomas et al. 2008; Abram et al. 2014a,b). For example, to construct a temperature-based proxy SAM index, Abram et al. (2014a) used the Marshall SAM index from 1957 to 1995 to calibrate each proxy record whose r value was then used to determine its weighted contribution to the reconstructed proxy SAM record.

To further investigate the temporal stability of the relationship between A_n (Fig. 5a) and the SAM (Fig. 5b) over the twentieth century, 11-yr running correlations (Fig. 5e) were calculated using the detrended time series of A_n and the Fogt SAM index (red). The relationship is intriguing as it elucidates two rapid and dramatic changes in the sign of the A_n–SAM relationship, one in the late 1940s and another in the mid-1970s. These transitions are contemporaneous with the well-documented change in the PDO from a warm phase to a cool phase in the North Pacific and later back to a warm phase (Fig. 5c). Although many (but not all) of the r values do not exceed 0.52 (required for $p < 0.1$), the rapidity of the transitions, their timing relative to a well-documented change in SSTs in the Pacific basin, and the sustained (multidecadal) nature of the event all argue against its origination as a random (chance) occurrence in the record. Although the other available SAM records (Fig. 6a), including the Abram et al. (2014a,b) proxy record, are not completely independent, each contains a contemporaneous rapid and multidecadal change in its correlation with A_n on the BP between the late 1940s and the mid-1970s (Fig. 6b).

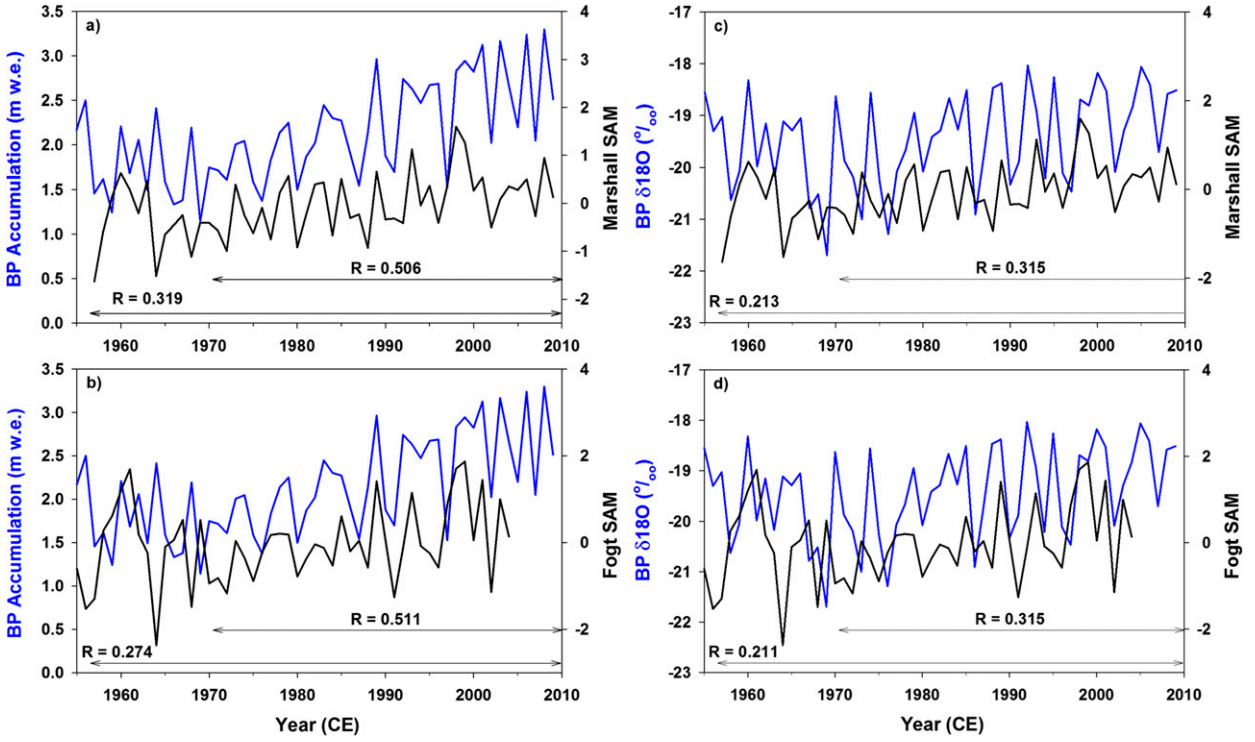

FIG. 4. Correlations between (a),(b) annual net accumulation and (c),(d) annual δ^{18}O on the BP and the (top) Marshall SAM index and (bottom) Fogt SAM index. The *r* values are shown for two time periods: the full record back to 1957 and a shorter interval back to 1971 that approximates the transition from the PDO warm to the PDO cold phase during which the correlations weaken. All correlations are based on detrended data and are shown in Table 1.

ENSO and SAM have been shown to interact on intraseasonal time scales (L'Heureux and Thompson 2006; Fogt et al. 2011) and ENSO teleconnections between the tropics and the South Pacific–Drake Passage region have been demonstrated although the strength of their interaction varies on decadal time scales (Fogt and Bromwich 2006). The correlation (1905–2005) between annual values of SOI (Fig. 5d) and A_n on the BP (Fig. 5e, black line), performed identically to that for the SAM, yields an *r* value of 0.13 ($p = 0.204$), weaker than that for the A_n–SAM relationship ($r = 0.279$, $p = 0.005$). Although the strength of the relationship varies over time, it is nearly always positive. However, the striking feature is the marked strengthening of the relationship from the late 1940s to the early 1970s during which the *r* values consistently exceed 0.52 ($p < 0.1$). This is the same period during which the A_n–SAM relationship (red line) changes sign and the PDO is in a sustained negative (cool) phase (Fig. 5f). Figures 5 and 6 highlight the synchronicity of these behavioral changes. These data suggest that the relationship between BP A_n and the SAM/SOI differs during periods of negative versus positive PDO conditions, and they likely play stronger or weaker roles at different times such that their interactions with the SAM change over time.

To investigate further the influence of PDO variability on the climate of the AP, spatial correlations were calculated between BP A_n and global SSTs, with both datasets detrended. Changepoint analysis (section 2h) of the A_n–SAM 11-yr running correlations identified two changepoints that break the time series into three intervals (1900–49, 1950–73, and 1974–2009). The mean of the 11-yr running correlations is 0.260 for the early period (prior to 1950), −0.424 for the middle period (1950–73), and 0.448 for the recent period (1974–2009).

TABLE 1. Correlations (*p* values) based on the detrended time series for the BP A_n and δ^{18}O and the Marshall (1957–2009) and Fogt (1957–2005) SAM indices. Values in boldface indicate 95% significance.

	Marshall–A_n	Marshall–δ^{18}O	Fogt–A_n	Fogt–δ^{18}O
1971–2009(05)	**0.506** ($p < 0.001$)	0.315 ($p = 0.051$)	**0.511** ($p = 0.002$)	0.315 ($p = 0.066$)
1957–2009(05)	**0.319** ($p = 0.020$)	0.213 ($p = 0.125$)	0.274 ($p = 0.056$)	0.211 ($p = 0.144$)

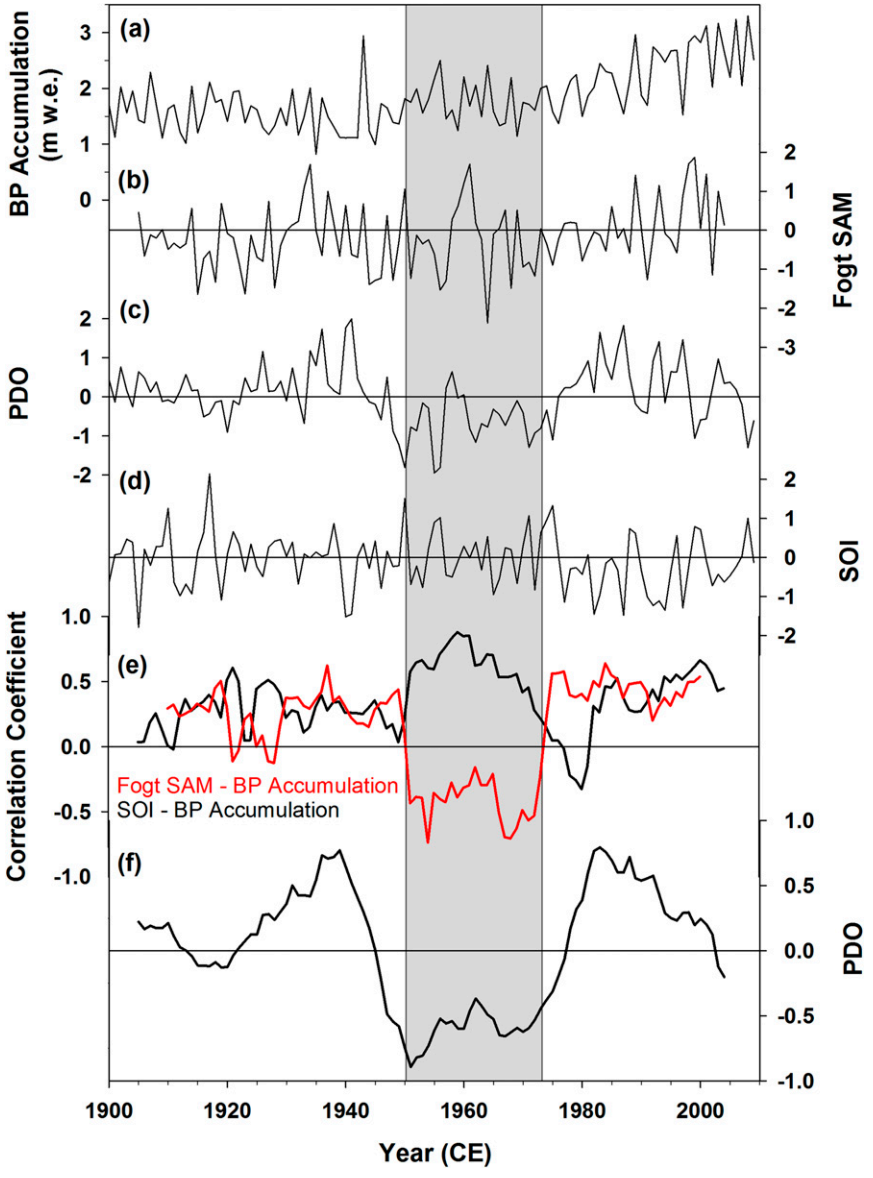

FIG. 5. Annual values of (a) net accumulation on the BP, (b) the Fogt SAM index, (c) the PDO, and (d) the SOI are shown with (e) 11-yr running correlations between the BP A_n and the Fogt SAM index (red) and the SOI (black) calculated using detrended data and (f) the 11-yr running mean of the PDO. Shading indicates the time between the changepoints, 1950 and 1973, calculated by changepoint analysis (section 2h), used in the correlation between BP A_n and the Fogt SAM index.

A two-tailed Student's t test of the means of the three periods reveals that they have statistically significant differences ($p < 0.001$), indicating that the changepoint analysis identified statistically significant shifts in the time series.

For the early period (1900–49), BP A_n shows positive and weak (insignificant) correlations to both the SAM and SOI (Fig. 5e), and the PDO shifts from near neutral (average: 0.06) to positive (average: 0.32) after 1925. Figure 7a reveals no significant tropical Pacific influence over the AP during the early period. Negative correlations exist between accumulation and SSTs in the Atlantic Ocean and become positive east of the AP, although the reliability of southern high-latitude SSTs is subject to uncertainty. The Fogt SAM index was generally negative at this time with a brief, strong positive excursion in the 1930s (Fig. 6a). Weaker westerlies and a weaker ASL associated with a negative SAM (Turner et al. 2013) would inhibit precipitation from the

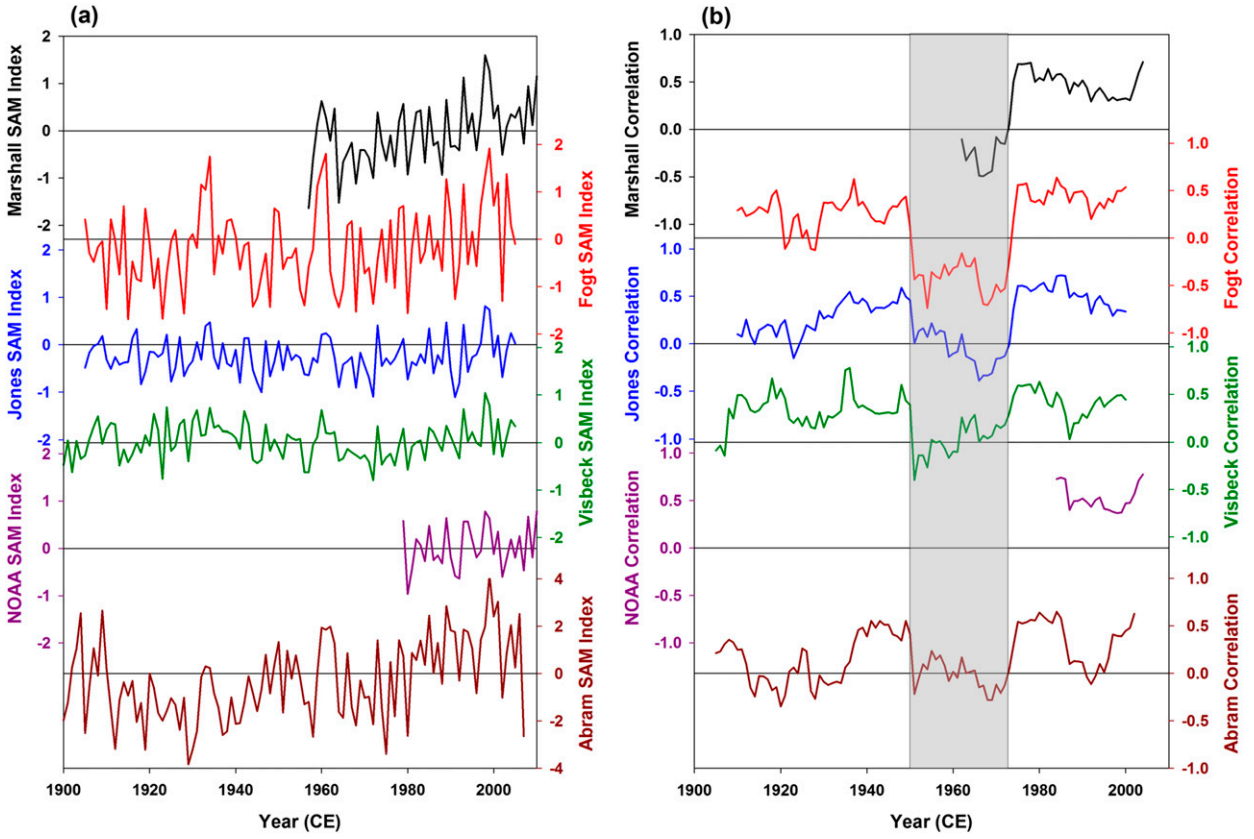

FIG. 6. (a) Six SAM indices and (b) their 11-yr running correlation with BP A_n. All correlations are calculated using detrended data. Shading indicates the time interval between the changepoints, 1950 and 1973, calculated by changepoint analysis (section 2h), used in the correlation between BP A_n and the Fogt SAM index.

western sources reaching the AP. Thus, moisture sources east of the AP may be more dominant when tropical forcing is weak and SAM is negative.

From 1950 to 1973, the PDO shifts to a strong negative phase (average: −0.57), and the relationship between BP A_n and the SAM (SOI) becomes distinctly negative (more strongly positive) (Fig. 5e). The SST correlations reveal less influence on BP A_n from local moisture sources around the AP; however, SSTs in the tropics and subtropics are strongly correlated with BP A_n (Fig. 7b). Positive correlations dominate the SPCZ region, far western Pacific, and central North Pacific. Negative correlations are evident along the equatorial Pacific, along the western coast of North America, and over the Indian Ocean. These patterns reflect both ENSO and the PDO, such that a La Niña event (positive SOI) accompanied by a negative PDO would enhance accumulation at the BP site.

After 1973, the relationship between BP A_n and the SAM becomes positive and the SAM begins an increasing trend to the present. The PDO is primarily positive (average: 0.27), and the A_n–SOI relationship fluctuates from negative around 1980 to weakly positive for the rest of the period. In this later period, the tropical influence on A_n is still present (Fig. 7c) but has shifted westward relative to the 1950–73 period. Negative correlations between BP A_n and SSTs are present around the continent except adjacent to the AP, particularly along the west coast. This supports the modern understanding of the SAM such that when the SAM is positive and the circumpolar westerlies are enhanced, the continent is rather isolated and colder. However, the enhanced westerlies tend to deepen the ASL, which has been demonstrated to be congruent with the trend in the PDO during SON as well (Clem and Fogt 2015), which increases northerly flow over the AP (Turner et al. 2013). This warm, moist northerly flow increases accumulation at the BP site. The tropical connection is still present such that a La Niña, and hence a southward shift in the SPCZ, would also serve to increase accumulation at the site. Again, SON trends in La Niña show increased MSLP in the southwest Atlantic, which also increases northerly onshore flow across the northwestern AP. Thus, in the future, if the current trends continue such that the SAM increases and

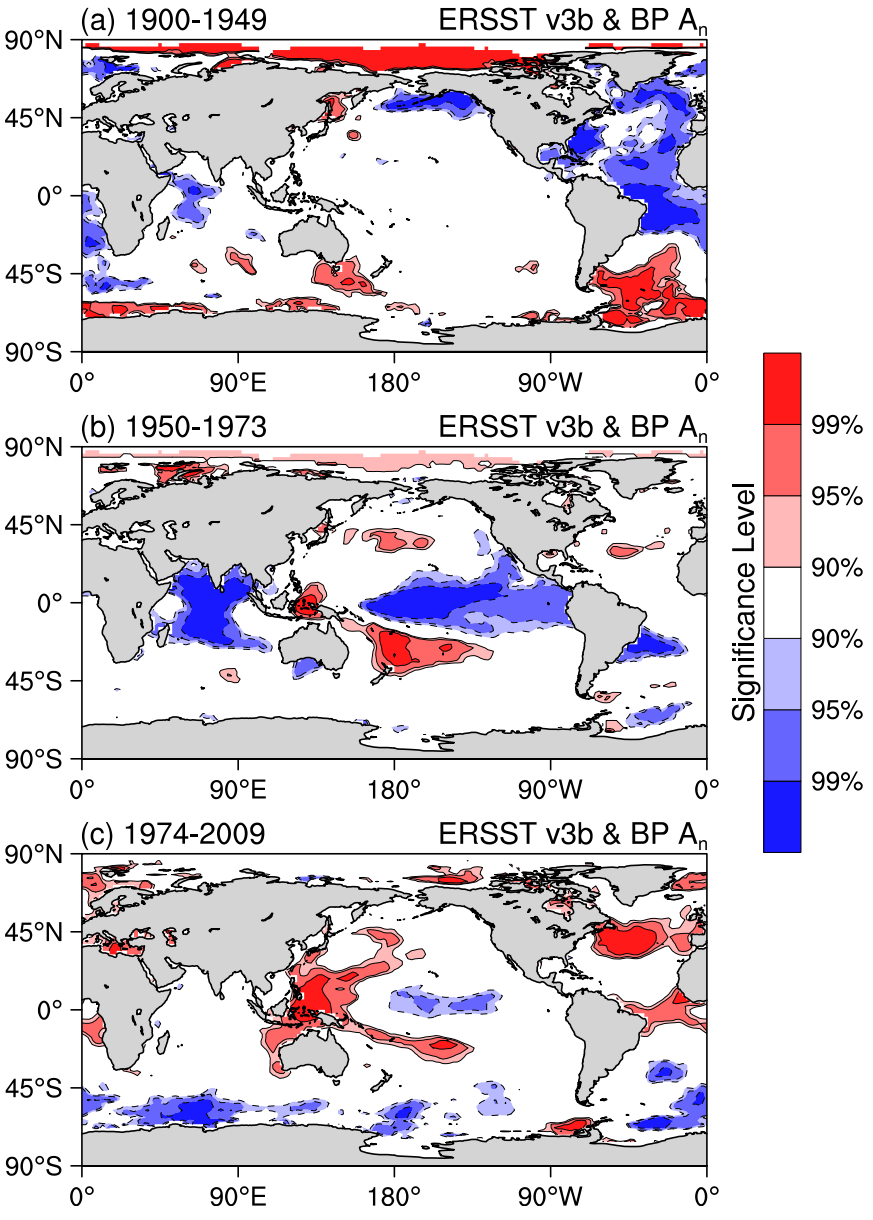

FIG. 7. Correlations between annual detrended BP A_n and SSTs from ERSST.v3b for (a) 1900–49, (b) 1950–73, and (c) 1974–2009. Positive (negative) correlations are shaded in red (blue) according to significance levels.

the PDO shifts toward a negative phase, high accumulation would be expected to continue at the BP site as well as over much of the northern AP.

4. Discussion

a. Interactions during the modern era (post 1957)

Having demonstrated that the A_n–SAM transitions are contemporaneous with phase changes in the PDO, a physical mechanism is proposed here to account for the changes. The SAM has shown an increasing trend since the 1970s but has only been persistently positive since the early 1990s. Under these persistently positive SAM conditions, the circumpolar westerlies are strong and located just north of Antarctica, thereby directing storms toward the AP. BP A_n also exhibits an increasing trend (0.327 m w.e. decade^{-1}) particularly since 1975 (Fig. 3a). During negative SAM conditions, the circumpolar storm track weakens considerably as the main westerly track relaxes northward toward Australia and New Zealand. These shifts in the circumpolar storm track are associated with the anomalous meridional

propagation of upper-level transient eddy momentum and baroclinicity inherent in SAM variability (Kidston et al. 2010; Fogt et al. 2011).

Since 1977, the PDO has been mostly positive although recently (post 1998) it has trended toward a negative phase. The positive PDO exhibits more El Niño–like conditions that shift the SPCZ to the northeast (in response to contracted Hadley circulation and a stronger subtropical jet stream), limiting poleward-propagating synoptic eddy momentum fluxes that can increase cyclonic activity near the AP (Chen et al. 1996). However, accumulation on the BP continued to increase during this period under the influence of the increasing SAM. Since 1999, atmospheric circulation has been dominated by the negative PDO phase wherein more La Niña–like conditions shift the SPCZ to the southwest, increasing the poleward synoptic eddy momentum fluxes (Vincent 1985). This shift, coupled with the strong circumpolar westerlies during a positive SAM, explains the ample precipitation on the AP since the turn of the twenty-first century as both the westerlies and poleward transient eddy momentum fluxes influence the region.

When both the SAM and the PDO are negative, the storm track associated with the SAM is pushed northward, inhibiting accumulation on the AP. Under this scenario, AP accumulation becomes more dependent on the poleward transient eddy momentum fluxes from the SPCZ, which are heavily influenced by ENSO (Fogt et al. 2011) and, by corollary, the PDO. This is bolstered by the dramatic shift toward negative A_n–SAM correlations and the concurrent strengthening of the A_n–SOI relationship from the mid-1940s to mid-1970s (Fig. 5e). Thus, the influence of tropical climate variability on AP accumulation is stronger when the circumpolar westerlies are less influential (i.e., weaker and northward as under negative SAM conditions). Given the uncertainties in reanalysis data for the SH prior to 1979 when negative SAM and negative PDO conditions were more prevalent, and the fact that conditions with both negative PDO and negative SAM have only occurred in two years since 1979, direct analysis of storm tracks under this scenario is severely limited. Atmospheric modeling of these conditions could provide further insights into the interactions of tropically influenced circumpolar storm tracks that help explain the relationship between the SAM and BP accumulation.

To test whether the PDO influence on the AP is independent of tropical ENSO effects, linear regression was used to remove the SOI from the PDO index. This technique does not entirely remove the ENSO signal from the PDO as their relationship is likely nonlinear, and in this case only the atmospheric component (SOI) is removed. Analysis of the PDO residuals (SOI linearly removed) regressed onto gridded SLP and OLR fields demonstrates its influence on the Southern Ocean and Antarctic continent from 1979 to 2012 when reanalysis data are most reliable in the SH. This time period was divided into two subsets to represent the dominant warm phase of the PDO (1979–98) and the recent shift toward a cold phase (1999–2012).

The influence of a warm phase PDO on the SLP and OLR is apparent in the NH but extremely limited in the SH (Figs. 8a,b). Linearly removing the PDO signal from the SOI time series isolates the ENSO-only tropical teleconnection to the AP (Figs. 8c,d,g,h). The SOI has a greater influence on the South Pacific than the PDO. The ASL region shows a negative relationship with the SOI (Fig. 8c) such that an El Niño event would increase ASL pressure, which would reduce BP A_n. In addition, during an El Niño event, convection would be situated over the equator and across southern South America (Fig. 8d). However, since 1999 the PDO has been predominantly negative (cold phase) under which these relationships are substantially different. Contemporaneously, the SLP in the Amundsen Sea region has been decreasing (Clem and Fogt 2015) in response to a negative trend in the PDO, an increasing SOI, and an increasing SAM. SLP regression indicates that a cold PDO phase would accompany lower SLP around the AP (Fig. 8e), although this relationship is not statistically significant. However, a significant (95%) positive relationship exists between the PDO and SLP in the western Pacific near the origin of the SPCZ. This is accompanied by a significant positive relationship between the PDO and OLR to the southwest of the long-term SPCZ position (Fig. 8f), which reflects increased convection and a southwest displacement of the SPCZ associated with a cold phase PDO. Thus the PDO acts on the SH independently of the SOI, supporting the results of Folland et al. (2002), who found that shifts in the position of the SPCZ are attributable to both ENSO and the IPO (a quasi-symmetric Pacific-wide manifestation of the PDO). During this cold phase, the relationships between the SOI and SLP (Fig. 8g) and OLR (Fig. 8h) are spatially similar to the prior warm phase (Figs. 8c,d) although somewhat enhanced. The SLP relationship is enhanced especially in the ASL region. Likewise, the negative relationship with OLR around the Antarctic continent and southwest of the SPCZ indicates that a La Niña event would accompany a southwest shift in the SPCZ and increased convection extending toward the AP (Fig. 8h). This period might be regarded to some degree as an analog for the 1950–73 period when tropical forcing appeared to exert more influence on BP A_n (Fig. 7b). This analysis demonstrates that both the PDO and the SOI independently influence the climate of the

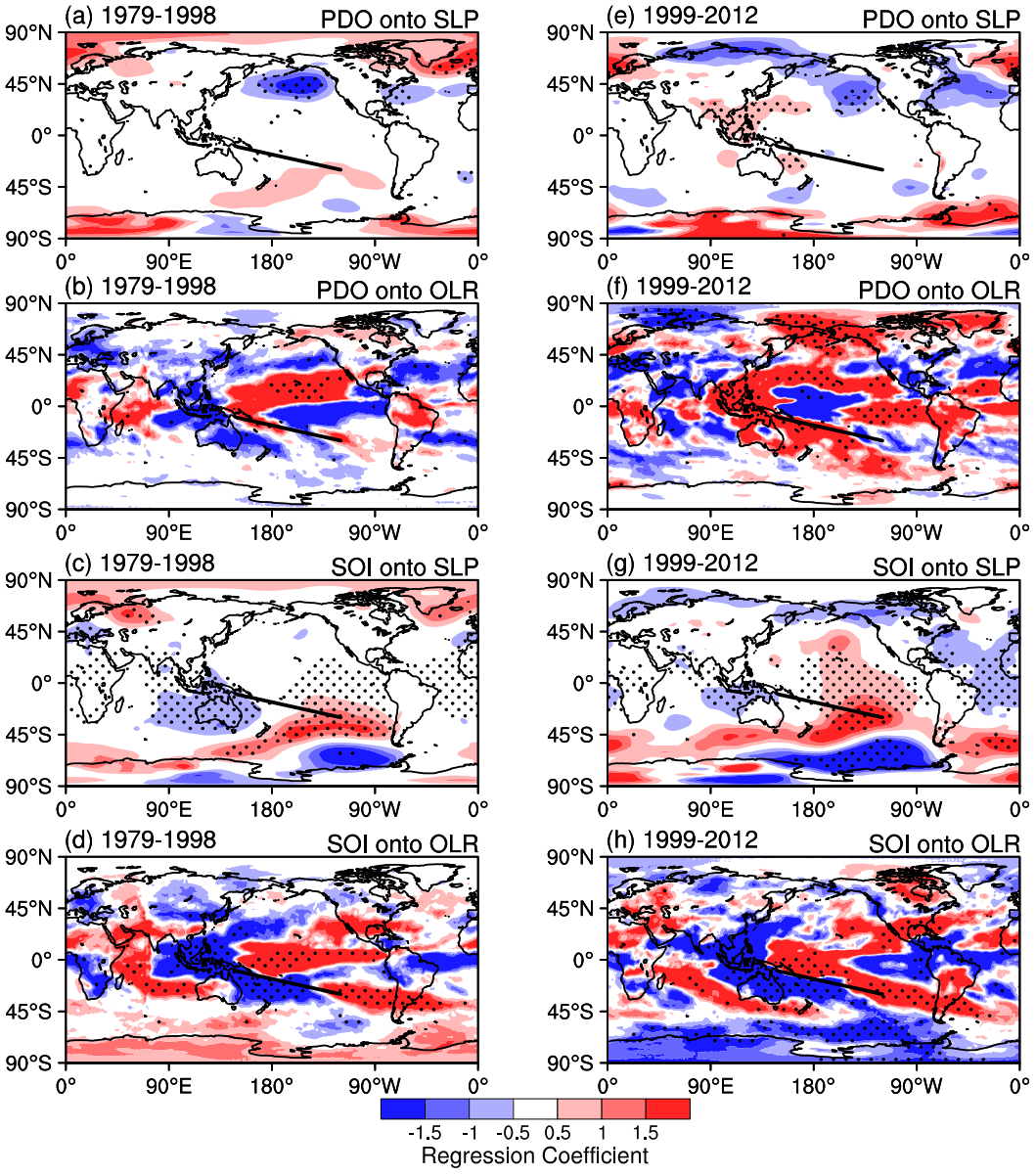

FIG. 8. Regression analysis for (left) 1979–98 and (right) 1999–2012 of the PDO with the SOI linearly removed onto (a),(e) SLP and (b),(f) OLR and of the SOI with the PDO linearly removed onto (c),(g) SLP and (d),(h) OLR. Stippling indicates 95% significance, and the mean position of the SPCZ (10°–30°S, 150°E–120°W) is represented by the black line.

AP during this most recent era (1979–2012) for which reliable data are available.

b. *Reconciling differences in the early records (pre 1957)*

Prior to 1950, differences in the correlations between various SAM reconstructions and BP A_n become more evident. The SAM indices (Fig. 6a) compare best over the post-1978 period when more and higher-quality data are available. An analysis by Jones et al. (2009) concluded that the station-based Marshall index best represents the SAM for the post-1957 period, which includes high-latitude station data. However, exploiting the longer ice core record requires a longer SAM history, which leaves the Fogt, Jones, Visbeck, and the newly developed Abram reconstructions. These indices are less reliable in the first half of the twentieth century due to data scarcity. Moreover, each reconstruction is based on different approaches. The reader is referred to the individual papers detailing the construction of each

index. However, some key comparisons should be noted. Despite the different methods and locations of data used, Fig. 6b clearly shows that all SAM indices (excluding NOAA) exhibit marked transitions in their correlations with BP A_n during the mid-1940s and mid-1970s, concomitant with PDO transitions. This further supports the PDO's role in modifying the relationship between the SAM and BP A_n.

The Abram SAM relationship with BP A_n is similar in nature to the other reconstructions from the mid-1960s to the early-1980s and prior to 1920 (Fig. 6b). However, the periodicity in the 11-yr running correlations with the BP A_n is markedly different for the Abram SAM index compared to the other longer records particularly during the 1930s and 1990s. During the 1930s, the Abram SAM correlations are muted (zero correlation) while the other indices exhibit a more positive relationship with BP A_n. Two explanations for this difference are put forth by Abram et al. (2014a), one questioning the linear detrending of the SAM and station observations of MSLP used in the Fogt SAM index (Jones et al. 2009) and the other noting the lack of high-latitude observations used in the Fogt SAM index. However, Jones et al. (2009) show that some of the seasonal differences between Fogt and Jones during the 1930s (note the positive peak evident in the annual Fogt time series as well; Fig. 6a) are largely due to station anomalies that are much stronger near New Zealand and weaker in South America. Therefore, these differences are more reflective of a regional SLP anomaly pattern than a hemispheric SAM and bear similarity to the TransPolar Index. This raises the question: Can the TPI also play a role in how the SAM indices, each created with different records, compare with BP A_n?

Figure 9 shows 11-yr running means of the Fogt and Abram SAM indices along with the TPI (Climatic Research Unit 1980), all of which have been standardized. Over the full period, the annual and 11-yr running mean Fogt index is more strongly correlated ($r = 0.45$, $p < 0.001$ and $r = 0.53$, $p < 0.001$, respectively) with the TPI than the Abram index ($r = 0.09$, $p = 0.373$ and $r = 0.23$, $p = 0.029$, respectively). This strong correlation between the Fogt index and the TPI stems from their close relationship during the period from 1920 to the mid-1950s as well as post-1980 (Fig. 9). During this time, the 11-yr running mean Abram index is significantly different from the Fogt index and the TPI. However, the Fogt and Abram indices are highly correlated from 1955 to 1979 ($r = 0.87$, $p < 0.001$). During this time, both indices are significantly anticorrelated with the TPI (Fogt: $r = -0.53$, $p = 0.007$; Abram: $r = -0.79$, $p < 0.001$) and the A_n–SAM relationship as well as the PDO are notably negative (Figs. 5e,f). This varying relationship between

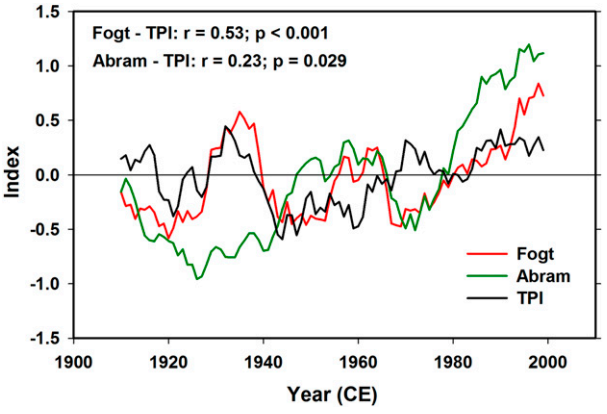

FIG. 9. The 11-yr running means of the Fogt (red) and Abram (green) SAM indices as well as the TPI (black) for 1905–2004.

different SAM indices and the TPI appears to be modulated by the phase of the PDO.

This draws into question the stability of proxy-based SAM reconstructions back in time, as different SAM indices may be more or less reflective of a circumpolar-natured SAM (i.e., Fogt index) compared to one that may be more regional (i.e., Abram index). As it applies to the BP A_n, the question becomes what is the main source of the precipitation? As mentioned previously, the dominant precipitation source for the BP is from the South Pacific Ocean. The accumulation is likely tied more to the regional SLP patterns that occur upstream from the Drake Passage. The Fogt index captures these regional SLP anomalies in the western Pacific that are part of the hemispheric nature of the SAM, thus reflecting a different relationship with A_n than the Abram index during certain periods. Therefore, care must be taken to ensure that the specific SAM index used reflects the climate variability of the study area in question, as differences in the regional versus hemispheric signals associated with each SAM index may skew the conclusions drawn concerning its relationship with various climate phenomena.

5. Conclusions

The relationship between BP A_n and large-scale atmospheric oscillations has not been temporally stable over the last century. The relationship between BP A_n and the SAM depends on the phase of both the SAM and the PDO. Tropical Pacific climate variability influences the accumulation on the AP more strongly under negative SAM conditions when the circumpolar westerlies are less influential (i.e., weaker and positioned farther northward). The BP A_n–SOI relationship is primarily positive but is stronger during negative PDO and negative SAM conditions. As the SAM becomes more positive, the BP A_n–SAM relationship also

becomes positive, and the BP A_n–SOI relationship weakens. These multidecadal characteristics of the accumulation–oscillation relationships are not apparent when data only from the post-1970s era are analyzed.

Running correlations between BP A_n and SAM show a sharp transition from positive to negative values between 1950 and 1973. During this time, the SAM ranges from negative to neutral, with one exception around the early 1960s when the SAM was briefly positive. The PDO was also in a negative phase and La Niña–like conditions were dominant. The reduced influence of the SAM on the accumulation over the AP allows tropical climate variability to exert a larger influence on accumulation. As the running correlations between SAM and accumulation weaken, the positive correlations between SOI and accumulation increase. These results support findings that the strength of the ENSO teleconnection to the South Pacific (Amundsen Sea and Drake Passage regions) is modulated by the SAM (Fogt et al. 2011), but they also suggest that the phase of the PDO is a modulating factor. More work is needed to understand the mechanisms through which the PDO modulates ENSO (Dong and Dai 2015), and modeling may help confirm how the position of the SPCZ affects the upper-level dynamics necessary for the generation of Rossby waves and their propagation throughout the SH (Garreaud and Battisti 1999; Clem and Renwick 2015).

This analysis has demonstrated the importance of using this new ice core–derived accumulation record to broaden the understanding of atmospheric circulation variability over the AP. The conventional view of the role of SAM and other climate oscillators has been derived primarily from post-1957 data, but this view is challenged by longer proxy records such as that from the BP ice core. Understanding how these complex forcings interact to control the transport of heat and mass (water vapor) and how they change over time hinges upon the use of these proxy records.

The SAM signal preserved in proxy records depends on the location from which the record is retrieved. Ice core sites around the AP exhibit sensitivity to the SAM differently (Thomas et al. 2008; Abram et al. 2014a), so individual sites must be investigated to determine the suitability of their records for SAM reconstructions. This may prove challenging as observational records necessary for calibration are limited in duration and spatial coverage. The results of this study may be applied to locations in the AP that are dominated by maritime westerly flow (western coast of the AP) and are situated in latitudes with significant SAM-induced variability in the strength of the circumpolar westerlies. Locations on the east coast (e.g., James Ross Island) or farther south (e.g., Gomez) have been shown to have different relationships between accumulation (or isotopes) and large-scale atmospheric oscillations, most specifically the SAM. The relationships described in this study will be easier to identify at sites with higher accumulation rates that allow clear identification of each year in the record. In the early twentieth century, the SAM indices, as well as the proxy-based reconstruction discussed, are not consistent due to the different locations of the sites whose data are incorporated in their respective models.

The relationships with accumulation on the BP discussed here suggest that other processes in addition to the SAM (e.g., the PDO and SOI) likely play stronger and weaker roles at different times such that their interactions with the SAM are not stationary. Accumulation on the BP is modulated by variability in the tropical and subtropical atmosphere through its impact on the strength and position of the circumpolar westerlies. If the processes and their interactions governing the temporal variability of accumulation on the BP during the twentieth century can be better elucidated, then the longer (~500 yr) annually resolved accumulation history available from the BP ice core might provide additional clues regarding the longer histories of these atmospheric oscillators.

Acknowledgments. The authors thank members of the BP field team [Victor Zagorodnov, Vladimir Mikhalenko, Benjamin Vicencio, Roberto Filippi (deceased), and Thai Verzoni], who spent 42 days with Ellen Mosley-Thompson drilling the BP ice cores. We thank Raytheon Polar Services and the British Antarctic Survey who provided essential logistical support of the field activities. Bradley P. Goodwin thanks The Ohio State University's Graduate School and Department of Geography and the National Science Foundation (NSF) for graduate student support. We thank Julie Jones for personally sending us her SAM reconstruction. Interpolated OLR and NCEP–NCAR reanalyses data were provided by NOAA/OAR/ESRL PSD from http://www.esrl.noaa.gov/psd/. The field project, laboratory analyses, and partial support for Bradley P. Goodwin were provided by NSF Award ANT-0732655 to Ellen Mosley-Thompson as part of NSF's IPY LARISSA Project. The ice core data used in this study are archived in the Global Change Master Directory (http://gcmd.nasa.gov/getdif.htm?LARISSA_0732655) and NOAA's National Climate Data Center/Paleoclimatology (http://www.ncdc.noaa.gov/data-access/paleoclimatology-data).

REFERENCES

Abram, N. J., E. R. Thomas, J. R. McConnell, R. Mulvaney, T. J. Bracegirdle, L. C. Sime, and A. J. Aristarain, 2010: Ice core

evidence for a 20th century decline of sea ice in the Bellingshausen Sea, Antarctica. *J. Geophys. Res.*, **115**, D23101, doi:10.1029/2010JD014644.

——, R. Mulvaney, and C. Arrowsmith, 2011: Environmental signals in a highly resolved ice core from James Ross Island, Antarctica. *J. Geophys. Res.*, **116**, D20116, doi:10.1029/2011JD016147.

——, E. W. Wolff, and M. A. J. Curran, 2013: A review of sea ice proxy information from polar ice cores. *Quat. Sci. Rev.*, **79**, 168–183, doi:10.1016/j.quascirev.2013.01.011.

——, R. Mulvaney, F. Vimeux, S. J. Phipps, J. Turner, and M. H. England, 2014a: Evolution of the southern annular mode during the past millennium. *Nat. Climate Change*, **4**, 564–569, doi:10.1038/nclimate2235.

——, ——, ——, ——, ——, and ——, 2014b: Southern annular mode (SAM) index 1000 year reconstruction. NOAA National Climatic Data Center, accessed 6 April, 2015. [Available online at ftp://ftp.ncdc.noaa.gov/pub/data/paleo/contributions_by_author/abram2014/abram2014sam.txt.]

Alexander, M. A., C. Deser, and M. S. Timlin, 1999: The reemergence of SST anomalies in the North Pacific Ocean. *J. Climate*, **12**, 2419–2433, doi:10.1175/1520-0442(1999)012<2419:TROSAI>2.0.CO;2.

Allan, R. J., N. Nicholls, P. D. Jones, and I. J. Butterworth, 1991: A further extension of the Tahiti–Darwin SOI, early ENSO events and Darwin pressure. *J. Climate*, **4**, 743–749, doi:10.1175/1520-0442(1991)004<0743:AFEOTT>2.0.CO;2.

Andreoli, R. V., and M. T. Kayano, 2005: ENSO-related rainfall anomalies in South America and associated circulation features during warm and cold Pacific decadal oscillation regimes. *Int. J. Climatol.*, **25**, 2017–2030, doi:10.1002/joc.1222.

Chen, B., S. R. Smith, and D. H. Bromwich, 1996: Evolution of the tropospheric split jet over the South Pacific Ocean during the 1986–89 ENSO cycle. *Mon. Wea. Rev.*, **124**, 1711–1731, doi:10.1175/1520-0493(1996)124<1711:EOTTSJ>2.0.CO;2.

Clem, K. R., and R. L. Fogt, 2013: Varying roles of ENSO and SAM on the Antarctic Peninsula climate in austral spring. *J. Geophys. Res. Atmos.*, **118**, 11 481–11 492, doi:10.1002/jgrd.50860.

——, and ——, 2015: South Pacific circulation changes and their connection to the tropics and regional Antarctic warming in austral spring, 1979–2012. *J. Geophys. Res.*, **120**, 2773–2792, doi:10.1002/2014JD022940.

——, and J. A. Renwick, 2015: Austral spring Southern Hemisphere circulation and temperature changes and links to the SPCZ. *J. Climate*, **28**, 7371–7384, doi:10.1175/JCLI-D-15-0125.1.

Climatic Research Unit, 1980: Trans Polar Index (TPI). University of East Anglia, accessed 31 December 2014. [Available online at http://www.cru.uea.ac.uk/cru/data/tpi/.]

——, 1987: Southern Oscillation Index (SOI). University of East Anglia, accessed 6 April, 2015. [Available online at http://www.cru.uea.ac.uk/cru/data/soi.]

Crozaz, G., 1969: Fission products in Antarctic snow: An additional reference level in January, 1965. *Earth Planet. Sci. Lett.*, **6**, 6–8, doi:10.1016/0012-821X(69)90152-6.

Curran, M. A. J., and G. B. Jones, 2000: Dimethyl sulfide in the Southern Ocean: Seasonality and flux. *J. Geophys. Res.*, **105** (D16), 20 451–20 459, doi:10.1029/2000JD900176.

——, T. D. van Ommen, V. I. Morgan, K. L. Phillips, and A. S. Palmer, 2003: Ice core evidence for Antarctic sea ice decline since the 1950s. *Science*, **302**, 1203–1206, doi:10.1126/science.1087888.

Dansgaard, W., and S. J. Johnsen, 1969: A flow model and a time scale for the ice core from Camp Century, Greenland. *J. Glaciol.*, **53**, 215–223.

Deser, C., A. S. Phillips, and J. W. Hurrell, 2004: Pacific interdecadal climate variability: Linkages between the tropics and the North Pacific during boreal winter since 1900. *J. Climate*, **17**, 3109–3124, doi:10.1175/1520-0442(2004)017<3109:PICVLB>2.0.CO;2.

Dethloff, K., K. Glushak, A. Rinke, and D. Handorf, 2010: Antarctic 20th century accumulation changes based on regional climate model simulations. *Adv. Meteor.*, **2010**, 327172, doi:10.1155/2010/327172.

Ding, Q., and E. J. Steig, 2013: Temperature change on the Antarctic Peninsula linked to the tropical Pacific. *J. Climate*, **26**, 7570–7585, doi:10.1175/JCLI-D-12-00729.1.

——, ——, D. S. Battisti, and M. Kuttel, 2011: Winter warming in West Antarctica caused by central tropical Pacific warming. *Nat. Geosci.*, **4**, 398–403, doi:10.1038/ngeo1129.

——, ——, ——, and J. M. Wallace, 2012: Influence of the tropics on the southern annular mode. *J. Climate*, **25**, 6330–6348, doi:10.1175/JCLI-D-11-00523.1.

Dong, B., and A. Dai, 2015: The influence of the interdecadal Pacific oscillation on temperature and precipitation over the globe. *Climate Dyn.*, **45**, 2667–2681, doi:10.1007/s00382-015-2500-x.

Eichler, T. P., and J. Gottschalck, 2013: A comparison of Southern Hemisphere cyclone track climatology and interannual variability in coarse-gridded reanalysis datasets. *Adv. Meteor.*, **2013**, 891260, doi:10.1155/2013/891260.

Fogt, R. L., 2007: Investigation of the southern annular mode and the El Niño–Southern Oscillation interactions. Ph.D. dissertation, The Ohio State University, 234 pp.

——, 2009: Seasonal Southern Hemisphere annular mode (SAM) reconstructions. Byrd Polar and Climate Research Center, accessed 6 April 2015. [Available online at http://polarmet.osu.edu/ACD/sam/sam_recon.html.]

——, and D. H. Bromwich, 2006: Decadal variability of the ENSO teleconnection to the high-latitude South Pacific governed by coupling with the southern annular mode. *J. Climate*, **19**, 979–997, doi:10.1175/JCLI3671.1.

——, J. Perlwitz, A. J. Monaghan, D. H. Bromwich, J. M. Jones, and G. J. Marshall, 2009: Historical SAM variability. Part II: 20th century variability and trends from reconstructions, observations, and the IPCC AR4 models. *J. Climate*, **22**, 5346–5365, doi:10.1175/2009JCLI2786.1.

——, D. H. Bromwich, and K. M. Hines, 2011: Understanding the SAM influence on the South Pacific ENSO teleconnection. *Climate Dyn.*, **36**, 1555–1576, doi:10.1007/s00382-010-0905-0.

——, A. J. Wovrosh, R. A. Langen, and I. Simmonds, 2012: The characteristic variability and connection to the underlying synoptic activity of the Amundsen–Bellingshausen Seas low. *J. Geophys. Res.*, **117**, D07111, doi:10.1029/2011JD017337.

Folland, C. K., D. E. Parker, A. Colman, and R. Washington, 1999: Large scale modes of ocean surface temperature since the late nineteenth century. *Beyond El Nino: Decadal and Interdecadal Climate Variability*, A. Navarra, Ed., Springer-Verlag, 73–102.

——, J. A. Renwick, M. J. Salinger, and A. B. Mullan, 2002: Relative influences of the interdecadal Pacific oscillation and ENSO on the South Pacific convergence zone. *Geophys. Res. Lett.*, **29** (13), doi:10.1029/2001GL014201.

Garreaud, R. D., and D. S. Battisti, 1999: Interannual (ENSO) and interdecadal (ENSO-like) variability in the Southern

Hemisphere tropospheric circulation. *J. Climate*, **12**, 2113–2123, doi:10.1175/1520-0442(1999)012<2113:IEAIEL>2.0.CO;2.

Gong, D., and S. Wang, 1999: Definition of Antarctic oscillation index. *Geophys. Res. Lett.*, **26**, 459–462, doi:10.1029/1999GL900003.

Gong, T., S. B. Feldstein, and D. Luo, 2010: The impact of ENSO on wave breaking and southern annular mode events. *J. Atmos. Sci.*, **67**, 2854–2870, doi:10.1175/2010JAS3311.1.

——, ——, and ——, 2013: A simple GCM study on the relationship between ENSO and the southern annular mode. *J. Atmos. Sci.*, **70**, 1821–1832, doi:10.1175/JAS-D-12-0161.1.

Gregory, S., and D. Noone, 2008: Variability in the teleconnection between the El Niño–Southern Oscillation and West Antarctic climate deduced from West Antarctic ice core isotope records. *J. Geophys. Res.*, **113**, D17110, doi:10.1029/2007JD009107.

Hansen, J., R. Ruedy, J. Glascoe, and M. Sato, 1999: GISS analysis of surface temperature change. *J. Geophys. Res.*, **104** (D24), 30 997–31 022, doi:10.1029/1999JD900835.

Hosking, J. S., A. Orr, G. J. Marshall, J. Turner, and T. Phillips, 2013: The influence of the Amundsen–Bellingshausen Seas low on the climate of West Antarctica and its representation in coupled climate model simulations. *J. Climate*, **26**, 6633–6648, doi:10.1175/JCLI-D-12-00813.1.

Jones, J. M., R. L. Fogt, M. Widmann, G. Marshall, P. D. Jones, and M. Visbeck, 2009: Historical SAM variability, Part I: Century length seasonal reconstructions. *J. Climate*, **22**, 5319–5345, doi:10.1175/2009JCLI2785.1.

Jones, P. D., M. J. Salinger, and A. B. Mullan, 1999: Extratropical circulation indices in the Southern Hemisphere based on station data. *Int. J. Climatol.*, **19**, 1301–1317, doi:10.1002/(SICI)1097-0088(199910)19:12<1301::AID-JOC425>3.0.CO;2-P.

Kalnay, E., and Coauthors, 1996: The NCEP/NCAR 40-Year Reanalysis Project. *Bull. Amer. Meteor. Soc.*, **77**, 437–471, doi:10.1175/1520-0477(1996)077<0437:TNYRP>2.0.CO;2.

Kang, S. M., L. M. Polvani, J. C. Fyfe, and M. Sigmond, 2011: Impact of polar ozone depletion on subtropical precipitation. *Science*, **332**, 951–954, doi:10.1126/science.1202131.

Kidston, J., D. M. W. Frierson, J. A. Renwick, and G. K. Vallis, 2010: Observations, simulations, and dynamics of jet stream variability and annular modes. *J. Climate*, **23**, 6186–6199, doi:10.1175/2010JCLI3235.1.

Killick, R., and I. A. Eckley, 2014: changepoint: An R package for changepoint analysis. *J. Stat. Softw.*, **58**, 1–19, doi:10.18637/jss.v058.i03.

King, J. C., 1994: Recent climate variability in the vicinity of the Antarctic Peninsula. *Int. J. Climatol.*, **14**, 357–369, doi:10.1002/joc.3370140402.

Können, G. P., P. D. Jones, M. H. Kaltofen, and R. J. Allan, 1998: Pre-1866 extensions of the Southern Oscillation Index using early Indonesian and Tahitian meteorological readings. *J. Climate*, **11**, 2325–2339, doi:10.1175/1520-0442(1998)011<2325:PEOTSO>2.0.CO;2.

Lee, H.-T., 2014: Climate Algorithm Theoretical Basis Document (C-ATBD): Outgoing longwave radiation (OLR)—Daily. NOAA's climate data record (CDR) program. CDRP-ATBD-0526, 46 pp.

Lee, S.-K., C. Wang, and B. E. Mapes, 2009: A simple atmospheric model of the local and teleconnection responses to tropical heating anomalies. *J. Climate*, **22**, 272–284, doi:10.1175/2008JCLI2303.1.

L'Heureux, M. L., and D. W. J. Thompson, 2006: Observed relationships between the El Niño–Southern Oscillation and the extratropical zonal-mean circulation. *J. Climate*, **19**, 276–287, doi:10.1175/JCLI3617.1.

Mantua, N. J., 1997: PDO Index. University of Washington, accessed 6 April 2015. [Available online at http://jisao.washington.edu/pdo/PDO.latest.]

——, S. R. Hare, Y. Zhang, J. M. Wallace, and R. C. Francis, 1997: A Pacific interdecadal climate oscillation with impacts on salmon production. *Bull. Amer. Meteor. Soc.*, **78**, 1069–1079, doi:10.1175/1520-0477(1997)078<1069:APICOW>2.0.CO;2.

Marshall, G. J., 2002: Trends in Antarctic geopotential height and temperature: A comparison between radiosonde and NCEP–NCAR reanalysis data. *J. Climate*, **15**, 659–674, doi:10.1175/1520-0442(2002)015<0659:TIAGHA>2.0.CO;2.

——, 2003a: Trends in the southern annular mode from observations and reanalyses. *J. Climate*, **16**, 4134–4143, doi:10.1175/1520-0442(2003)016<4134:TITSAM>2.0.CO;2.

——, 2003b: An observation-based Southern Hemisphere annular mode index. British Antarctic Survey, accessed on 6 April 2015. [Available online at http://www.nerc-bas.ac.uk/icd/gjma/sam.html.]

——, V. Lagun, and T. A. Lachlan-Cope, 2002: Changes in Antarctic Peninsula tropospheric temperatures from 1956 to 1999: A synthesis of observations and reanalysis data. *Int. J. Climatol.*, **22**, 291–310, doi:10.1002/joc.758.

——, A. Orr, N. P. M. van Lipzig, and J. C. King, 2006: The impact of a changing Southern Hemisphere annular mode on Antarctic Peninsula summer temperatures. *J. Climate*, **19**, 5388–5404, doi:10.1175/JCLI3844.1.

——, ——, and J. Turner, 2013: A predominant reversal in the relationship between the SAM and East Antarctic temperatures during the twenty-first century. *J. Climate*, **26**, 5196–5204, doi:10.1175/JCLI-D-12-00671.1.

Mercer, J. H., 1978: West Antarctic ice sheet and CO_2 greenhouse effect: A threat of disaster. *Nature*, **271**, 321–325, doi:10.1038/271321a0.

Mo, K. C., 2000: Relationships between low-frequency variability in the Southern Hemisphere and sea surface temperature anomalies. *J. Climate*, **13**, 3599–3610, doi:10.1175/1520-0442(2000)013<3599:RBLFVI>2.0.CO;2.

Mulvaney, R., and Coauthors, 2012: Recent Antarctic Peninsula warming relative to Holocene climate and ice-shelf history. *Nature*, **489**, 141–144, doi:10.1038/nature11391.

Newman, M., G. P. Compo, and M. A. Alexander, 2003: ENSO-forced variability of the Pacific decadal oscillation. *J. Climate*, **16**, 3853–3857, doi:10.1175/1520-0442(2003)016<3853:EVOTPD>2.0.CO;2.

NOAA, 2000: Antarctic Oscillation. NOAA Climate Prediction Center, accessed 6 April 2015. [Available online at http://www.cpc.ncep.noaa.gov/products/precip/CWlink/daily_ao_index/aao/aao.shtml.]

Orr, A., D. Cresswell, G. Marshall, J. Hunt, J. Sommeria, C. Wang, and M. Light, 2004: A "low-level" explanation for the recent large warming trend over the western Antarctic Peninsula involving blocked winds and changes in zonal circulation. *Geophys. Res. Lett.*, **31**, L06204, doi:10.1029/2003GL019160.

Pittock, A. B., 1980: Patterns of climatic variation in Argentina and Chile, I: Precipitation, 1931–60. *Mon. Wea. Rev.*, **108**, 1347–1361, doi:10.1175/1520-0493(1980)108<1347:POCVIA>2.0.CO;2.

——, 1984: On the reality, stability and usefulness of Southern Hemisphere teleconnections. *Aust. Meteor. Mag.*, **32**, 75–82.

Pourchet, M., F. Pinglot, and C. Lorius, 1983: Some meteorological applications of radioactive fallout measurements in Antarctic

snows. *J. Geophys. Res.*, **88** (C10), 6013–6020, doi:10.1029/JC088iC10p06013.

Power, S., T. Casey, C. Folland, A. Colman, and V. Mehta, 1999: Inter-decadal modulation of the impact of ENSO on Australia. *Climate Dyn.*, **15**, 319–324, doi:10.1007/s003820050284.

Preunkert, S., M. Legrand, B. Jourdain, C. Moulin, S. Belviso, N. Kasamatsu, M. Fukuchi, and T. Hirawake, 2007: Interannual variability of dimethylsulfide in air and seawater and its atmospheric oxidation by-products (methanesulfonate and sulfate) at Dumont d'Urville, coastal Antarctica (1999–2003). *J. Geophys. Res.*, **112**, D06306, doi:10.1029/2006JD007585.

Ropelewski, C. F., and P. D. Jones, 1987: An extension of the Tahiti–Darwin Southern Oscillation Index. *Mon. Wea. Rev.*, **115**, 2161–2165, doi:10.1175/1520-0493(1987)115<2161:AEOTTS>2.0.CO;2.

Sardeshmukh, P., and B. J. Hoskins, 1988: The generation of global rotational flow by steady idealized tropical divergence. *J. Atmos. Sci.*, **45**, 1228–1251, doi:10.1175/1520-0469(1988)045<1228:TGOGRF>2.0.CO;2.

Scambos, T. A., J. A. Bohlander, C. A. Shuman, and P. Skvarca, 2004: Glacier acceleration and thinning after ice shelf collapse in the Larsen B embayment, Antarctica. *J. Geophys. Res.*, **31**, L18402, doi:10.1029/2004GL020670.

SCAR, 2004: Antarctic climate data: Results from the SCAR READER Project. British Antarctic Survey, accessed 15 May 2014. [Available online at http://www.antarctica.ac.uk/met/READER/.]

Schneider, D. P., E. J. Steig, and J. C. Comiso, 2004: Recent climate variability in Antarctica from satellite-derived temperature data. *J. Climate*, **17**, 1569–1583, doi:10.1175/1520-0442(2004)017<1569:RCVIAF>2.0.CO;2.

——, Y. Okumura, and C. Deser, 2012: Observed Antarctic interannual climate variability and tropical linkages. *J. Climate*, **25**, 4048–4066, doi:10.1175/JCLI-D-11-00273.1.

Schneider, N., and B. D. Cornuelle, 2005: The forcing of the Pacific decadal oscillation. *J. Climate*, **18**, 4355–4372, doi:10.1175/JCLI3527.1.

Silvestri, G., and C. Vera, 2009: Nonstationary impacts of the southern annular mode on Southern Hemisphere climate. *J. Climate*, **22**, 6142–6148, doi:10.1175/2009JCLI3036.1.

Sime, L. C., G. J. Marshall, R. Mulvaney, and E. R. Thomas, 2009: Interpreting temperature information from ice cores along the Antarctic Peninsula: ERA-40 analysis. *Geophys. Res. Lett.*, **36**, L18801, doi:10.1029/2009GL038982.

Simpkins, G. R., L. M. Ciasto, D. W. J. Thompson, and M. H. England, 2012: Seasonal relationships between large-scale climate variability and Antarctica sea ice concentration. *J. Climate*, **25**, 5451–5469, doi:10.1175/JCLI-D-11-00367.1.

Smith, T. M., and R. W. Reynolds, 2002: Extended reconstruction of global sea surface temperatures based on COADS data (1854–1997). International Research Institute for Climate and Society, accessed 11 December 2014. [Available online at http://iridl.ldeo.columbia.edu/SOURCES/.NOAA/.NCDC/.ERSST/.version3b.]

——, ——, T. C. Peterson, and J. M. Lawrimore, 2008: Improvements to NOAA's historical merged land–ocean surface temperature analysis (1880–2006). *J. Climate*, **21**, 2283–2296, doi:10.1175/2007JCLI2100.1.

Stammerjohn, S. E., D. G. Martinson, R. C. Smith, X. Yuan, and D. Rind, 2008: Trends in Antarctic annual sea ice retreat and advance and their relation to El Niño–Southern Oscillation and southern annular mode variability. *J. Geophys. Res.*, **113**, C03S90, doi:10.1029/2007JC004269.

Thomas, E. R., G. J. Marshall, and J. R. McConnell, 2008: A doubling in snow accumulation in the western Antarctic Peninsula since 1850. *Geophys. Res. Lett.*, **35**, L01706, doi:10.1029/2007GL032529.

——, P. F. Dennis, T. J. Bracegirdle, and C. Franzke, 2009: Ice core evidence for significant 100-year regional warming on the Antarctic Peninsula. *Geophys. Res. Lett.*, **36**, L20704, doi:10.1029/2009GL040104.

Thompson, D. W. J., and J. M. Wallace, 2000: Annular modes in the extratropical circulation. Part I: Month-to-month variability. *J. Climate*, **13**, 1000–1016, doi:10.1175/1520-0442(2000)013<1000:AMITEC>2.0.CO;2.

——, and S. Solomon, 2002: Interpretation of recent Southern Hemisphere climate change. *Science*, **296**, 895–899, doi:10.1126/science.1069270.

——, ——, P. J. Kushner, M. H. England, K. M. Grise, and D. J. Karoly, 2011: Signatures of the Antarctic ozone hole in Southern Hemisphere surface climate change. *Nat. Geosci.*, **4**, 741–749, doi:10.1038/ngeo1296.

Thompson, L. G., D. A. Peel, E. Mosley-Thompson, R. Mulvaney, J. Dai, P. N. Lin, M. E. Davis, and C. F. Raymond, 1994: Climate since AD 1510 on Dyer Plateau, Antarctic Peninsula: Evidence for recent climate change. *Ann. Glaciol.*, **20**, 420–426.

Trenberth, K. E., 1997: The definition of El Niño. *Bull. Amer. Meteor. Soc.*, **78**, 2771–2777, doi:10.1175/1520-0477(1997)078<2771:TDOENO>2.0.CO;2.

Turner, J., 2004: Review: The El Niño–Southern Oscillation and Antarctica. *Int. J. Climatol.*, **24**, 1–31, doi:10.1002/joc.965.

——, and Coauthors, 2004: The SCAR READER project: Toward a high-quality database of mean Antarctic meteorological observations. *J. Climate*, **17**, 2890–2898, doi:10.1175/1520-0442(2004)017<2890:TSRPTA>2.0.CO;2.

——, and Coauthors, 2005: Antarctic climate change during the last 50 years. *Int. J. Climatol.*, **25**, 279–294, doi:10.1002/joc.1130.

——, T. A. Lachlan-Cope, G. J. Marshall, E. M. Morris, R. Mulvaney, and W. Winter, 2002: Spatial variability of Antarctic Peninsula net surface mass balance. *J. Geophys. Res.*, **107**, 4173, doi:10.1029/2001JD000755.

——, T. Phillips, J. S. Hosking, G. J. Marshall, and A. Orr, 2013: The Amundsen Sea low. *Int. J. Climatol.*, **33**, 1818–1829, doi:10.1002/joc.3558.

Vincent, D. G., 1985: Cyclone development in the South Pacific convergence zone during FGGE, 10–17 January 1979. *Quart. J. Roy. Meteor. Soc.*, **111**, 155–172, doi:10.1002/qj.49711146706.

——, 1994: The South Pacific convergence zone (SPCZ): A review. *Mon. Wea. Rev.*, **122**, 1949–1970, doi:10.1175/1520-0493(1994)122<1949:TSPCZA>2.0.CO;2.

Visbeck, M., 2007: Annual, seasonal & regional SAM-index. GEOMAR: Helmholtz Centre for Ocean Research Kiel, accessed 6 April 2015. Available online at http://www.geomar.de/fileadmin/personal/fb1/po/mvisbeck/sam_annual.tab.]

——, 2009: A station-based southern annular mode index from 1884 to 2005. *J. Climate*, **22**, 940–950, doi:10.1175/2008JCLI2260.1.

Xue, Y., T. M. Smith, and R. W. Reynolds, 2003: Interdecadal changes of 30-yr SST normals during 1871–2000. *J. Climate*, **16**, 1601–1612, doi:10.1175/1520-0442-16.10.1601.

Zhang, Y., J. M. Wallace, and D. S. Battisti, 1997: ENSO-like interdecadal variability: 1900–93. *J. Climate*, **10**, 1004–1020, doi:10.1175/1520-0442(1997)010<1004:ELIV>2.0.CO;2.